EurJIC
European Journal of Inorganic Chemistry

A Journal of ChemPubSoc Europe

Accepted Article

Title: A Cyclic-RGD Dinuclear TbIII Macrocyclic Complex as a Tumor Integrin-Selective Luminescence Probe

Authors: C. Allen Chang, Ju-Chien Chia, and Syue-Liang Lin

To be cited as: *Eur. J. Inorg. Chem.* 10.1002/ejic.201800568

Link to VoR: http://dx.doi.org/10.1002/ejic.201800568

WILEY-VCH

A Cyclic-RGD Dinuclear Tb^{III} Macrocyclic Complex as a Tumor Integrin-Selective Luminescence Probe

C. Allen Chang[1,2,3]*, Ju-Chien Chia[1], Syue-Liang Lin[2,3]

[1] Department of Biomedical Imaging and Radiological Sciences, National Yang-Ming University, No. 155, Sec. 2, Li-Nong St., Beitou, Taipei, Taiwan, 112, R.O.C. E-mail: cachang@ym.edu.tw, Tel: +886-2-28267000 Ext. 7943, Fax: +886-2-28238311.

[2] Department of Biotechnology and Laboratory Science in Medicine, National Yang-Ming University

[3] Molecular Imaging Research Center, National Yang-Ming University.

* Corresponding author: C. Allen Chang, E-mail: cachang@ym.edu.tw, Homepage: http://birs-e.web.ym.edu.tw/files/11-1253-1501-1.php

Abstract

To develop small molecular integrin-selective luminescence imaging probes, we have prepared the binary dipicolinate (DPA) Tb^{III} dinuclear macrocyclic complex, Tb_2(cRGDfK-ODO2A-dimer)$(DPA)_2^{2-}$ or complex I, and reference ligands and Tb^{III} complexes which were purified by HPLC and characterized by NMR, mass spectrometry and luminescence spectroscopy. Luminescence titrations of the structural and bonding model Tb_2(*m*-ODO2A-dimer)$^{2+}$ complex by DPA^{2-} ion confirmed the molecular formula of the adduct was Tb_2(*m*-ODO2A-dimer)$(DPA)_2^{2-}$, and the first binary binding constant was determined to be log K_1 = 5.76. At pH 7.4, complex I showed 300 times luminescence enhancement at 544 nm (λ_{ex} = 278 nm) as compared to that without adding DPA, and was found to bind to $\alpha_v\beta_3$ integrin and human glioblastoma U87MG tumor cells in both specific and non-specific modes, *via* luminescence spectroscopic and confocal cell imaging competition studies. This makes complex I and its future optimized derivatives potentially feasible for preclinical bioimaging applications, particularly in the time-resolved mode.

Introduction

Integrins in tumor cells and tumor related vessels contribute to increased cell migration, invasion, proliferation, metastasis and survival.[1-5] Host cellular response to cancer including angiogenesis is also upregulated by integrins, especially the $\alpha_v\beta_3$ type. Thus, tumor theranostics by targeting tumor cells and their microenvironment *via* targeting $\alpha_v\beta_3$ integrin could be an effective strategy.[1,2,6-8] Among various potential theranostic candidates, the Arg-Gly-Asp (RGD) motif which has been found in fibrinogen, fibronectin, plasminogen, metalloprotease-2 and osteopontin[9] is a specific peptide that targets the over-expressed $\alpha_v\beta_3$ integrin of melanoma, glioblastoma and

pancreatic tumors and their microenvironment. Because linear RGD has a flexible conformation and is decomposed relatively easily,[10] cyclic RGD forms such as cRGDfK and cRGDfV with better bio-stability and stronger $\alpha_v\beta_3$ integrin binding ability have been recently used for biomedical applications.[11-13] Although a number of radiolabeled cyclic RGD derivatives are known,[14-17] few small molecular cyclic RGD derivatives have been reported as integrin selective luminescence imaging probes which could be potentially more convenient to use.[18-20]

In our translational medicine research program, to develop macrocyclic dinuclear trivalent lanthanide (Ln^{III}) complexes as luminescence imaging probes[21] in conjunction with the discovery of tumor targeting fusion protein drugs,[22,23] we have selected the cRGDfK peptide biomarker as a common delivery vehicle to the tumor cells. As luminescence probes, thermodynamically stable and kinetically inert Ln^{III} macrocyclic complexes are preferred as compared to their linear structural analogues, and their long emission lifetimes are often advantageous for use in the time-resolved mode.[24] However, because the electric dipole f-f transitions are Laporte forbidden with very low extinction coefficients, the employment of the antenna effect *via* ligand organic chromophores is often used to enhance the sensitized emission from the Ln^{III} center.[25,26] In addition, we decided to use the dinuclear Ln^{III} systems not only because of the possibly double luminescence signals as compared to mononuclear ones but also that various mixed metal dinuclear systems such as $Ln_1^{III}Ln_2^{III}$ and/or Ln^{III}/M systems could be prepared where M could be a transition metal ion to examine potential luminescence energy transfer properties and their applications. Mononuclear Ln^{III} systems that we have studied often did not offer this kind versatility for various applications.[27,28] To understand the fundamental coordination properties, the solution speciation, density functional theory (DFT) calculations, luminescence properties and promoted nitrophenyl-phosphate hydrolysis rates of the parent dinuclear Ln^{III}-*m*-ODO2A-dimer macrocyclic complexes (Ln_2L, Ln = La, Eu, Tb, Yb, Y; L = *m*-ODO2A-dimer) of the current studies have been reported.[21]

Recently, we have found that the newly prepared Tb_2(cRGDfK-ODO2A-dimer)$(DPA)_2^{2-}$ complex (abbreviated as complex I, DPA^{2-} is the dipicolinate ion, Scheme 1) was able to selectively bind $\alpha_v\beta_3$ integrin and the human glioblastoma U87MG tumor cells *via* luminescence spectroscopic and confocal cell imaging competition studies. This approach has a unique feature in that just employing the antenna effect using the ligand chromophore in the Tb_2(cRGDfK-ODO2A-dimer)$^{2+}$ was not sufficient for convenient luminescence imaging. However, by adding DPA^{2-} ions, the resulting complex I showed 300 times luminescence enhancement[29,30] which made it and future optimized derivatives potentially feasible for practical bioimaging applications. The results are reported in this paper.

10.1002/ejic.201800568

Scheme 1. The structural formula of the Tb_2(cRGDfK-ODO2A-dimer)$(DPA)_2^{2-}$ or complex I. ● = DPA^{2-} ion.

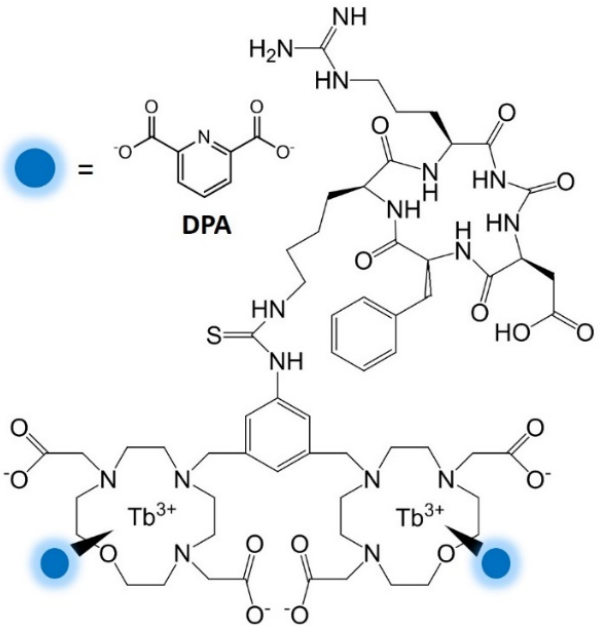

Results and Discussion

Synthesis of the ligands. The synthesis of various intermediates and macrocyclic ligands including the cRGDfK-ODO2A-dimer is outlined in Scheme 2. In brief, the coupling agent, 1,3-bis(bromomethyl)-5-nitrobenzene, was prepared from 5-nitroisophthalic acid via the intermediate 5-nitro-1,3-phenylene-dimethanol according to a published method.[31] Two equivalents of the compound, tricyclo[8,2,1,0]1-oxa-4,7,10-triazacyclotridecane (12N3O-tricyclic), prepared by a literature published method[32,33] were mixed with one equivalent of the coupling agent to result in 1,3-bis(1,4,10-triaza-7-oxacyclododec-1-ylmethyl)-5-nitrobenzene (nitro-12N3O-tricyclic-dimer). After alkylation and acidification, the compound, 1,3-bis[4,10-bis(carboxymethyl)-1,4,10-triaza-7-oxacyclododec-1-ylmethyl]-5-nitrobenzene hydrochloride salt (nitro-ODO2A-dimer HCl salt) was obtained. This compound was converted to 1,3-bis[4,10-bis(carboxymethyl)-1,4,10-triaza-7-oxacyclododec-1-ylmethyl]-5-aniline hydrochloride salt (amine-ODO2A-dimer HCl salt), and 1,3-bis[4, 10-bis(carboxy- methyl)-1,4,10-triaza-7-oxacyclododec-1-ylmethyl]-5-isothiocyanatobenzene hydrochloride salt (SCN-Bn-ODO2A-dimer, HCl salt) using published methods with minor modifications.[34] The SCN-Bn-ODO2A-dimer was further derivatized with cRGDfK peptide and glycine to obtain the respective cRGDfK-ODO2A-dimer and Gly-ODO2A-dimer.[35] For comparison and competition experiments, the compound cRGDfK-FITC (FITC = fluorescein isothiocyanate) was also synthesized. Selected NMR spectra, HPLC chromatograms and mass spectra of various intermediates and SCN-Bn-ODO2A-dimer derivatives are shown in the supporting information.

Scheme 2. The synthesis of the SCN-Bn-ODO2A-dimer and the cRGDfK-ODO2A-dimer.

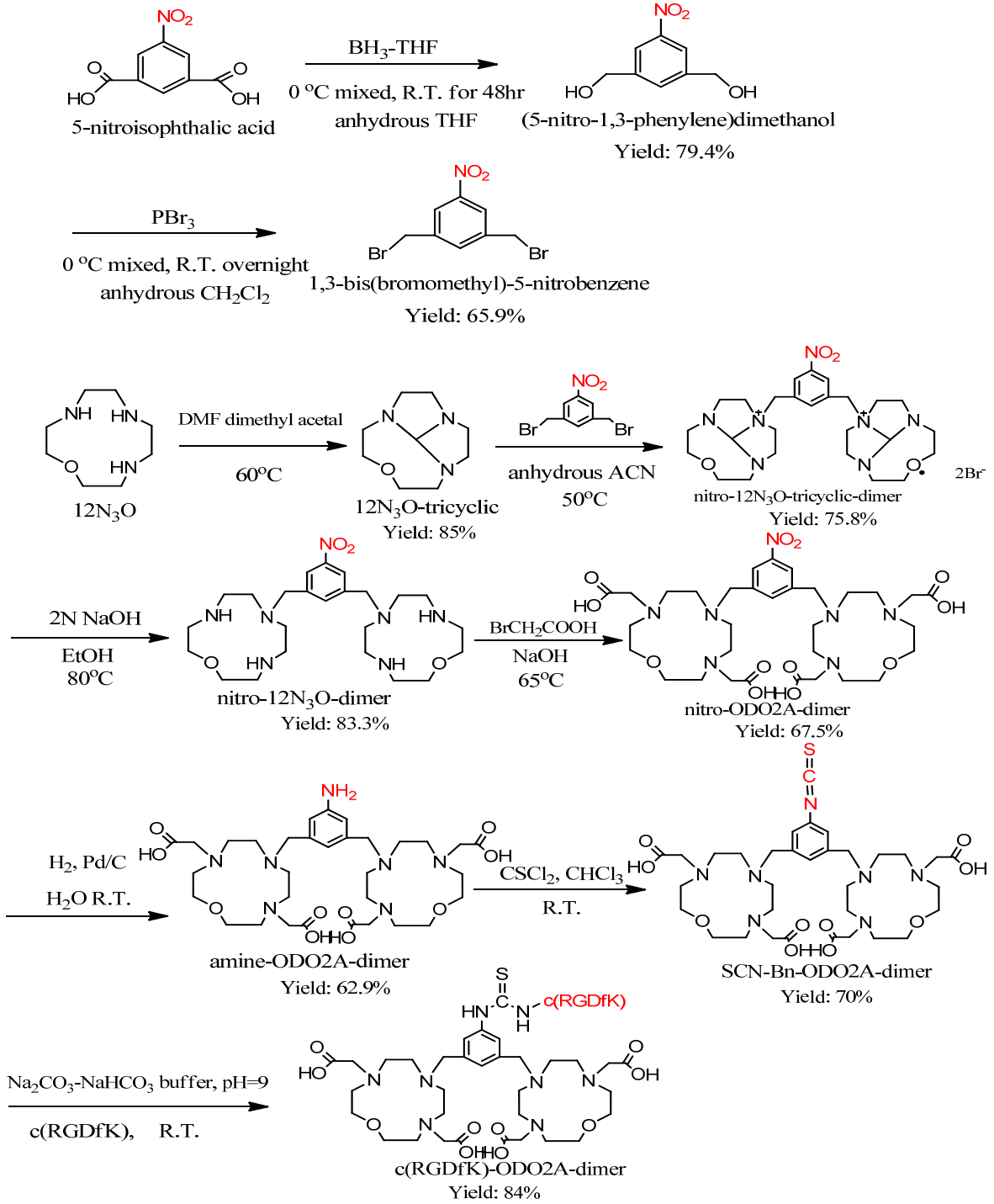

Luminescence studies. Solutions of Tb_2(cRGDfK-ODO2A-dimer) and complex I were prepared by mixing two equivalents of Tb^{III} ions with one equivalent of the appropriate ligand without or with additional two equivalents of DPA and the final mixtures were slowly adjusted to pH 7.4 using the 3-(N-morpholino) propanesulfonic acid (MOPS) buffer solution (0.10 M). Figure 1 showed the excitation (λ_{em} = 544 nm) and emission (λ_{ex} = 278 nm) spectra of the Tb_2(cRGDfK-ODO2A-dimer) at pH 7.4 (MOPS buffer). Excitation at 278 nm gave a typical Tb^{III} emission

spectrum with typical peaks at 490 nm ($^5D_4 \rightarrow {}^7F_6$), 544 nm ($^5D_4 \rightarrow {}^7F_5$), 584 nm ($^5D_4 \rightarrow {}^7F_4$) and 620 nm ($^5D_4 \rightarrow {}^7F_3$). Owing to the antenna effect, the luminescence signal at 544 nm is about 35 times greater than that excited directly at 355 nm without the antenna effect (data not shown).

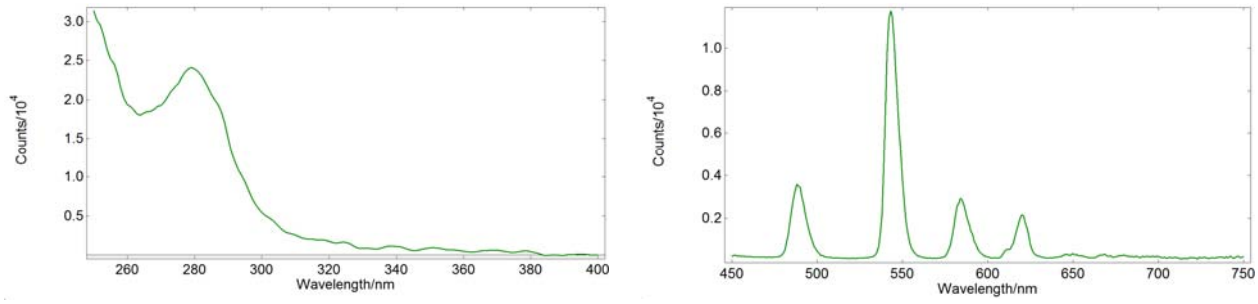

Figure 1. The excitation (λ_{em}=544 nm, left) and emission (λ_{ex}=278 nm, right) spectra of Tb_2(cRGDfK-ODO2A-dimer), 0.1 mM, pH 7.4, MOPS buffer.

Figure 2 showed the excitation (λ_{em} = 544 nm) and emission (λ_{ex} = 278 nm) spectra of the complex I (pH 7.4). As shown in Figure 2, the emission peak intensity at 544 nm increased another 300 times as compared to that of the Tb_2(cRGDfK-ODO2A-dimer) which was mainly due to the direct DPA^{2-} ion coordination in addition to displacement of inner-sphere coordinated water molecules (q) by the DPA^{2-} ions. The former was similar to the result of the ancillary ligand antenna effect,[29] i.e. the coordinated DPA^{2-} ion was closer to the Tb^{III} ion with a better energy level overlap than the substituted benzene ligand backbone. The latter was manifested by the increased lifetime of the Tb^{III} ion from 1.32 ms (without DPA, q = 1.6~2.0) to 2.49 ms (with DPA, q = 0.6) in the complex.[28] The luminescence decay curves of the Tb_2(cRGDfK-ODO2A-dimer) without and with DPA, and the estimation of the number of coordinated water molecules, q (λ_{ex} = 278 nm, λ_{em} = 540 nm; pH 7.4, MOPS buffer), were shown in the Supporting information, Figure S1 and Table S1, respectively. Note that removal of coordinated water molecules (i.e. O-H oscillators) only increased the luminescence intensity in smaller amount, normally not as high as 300 times enhancement, as shown in a previously published paper when pH was raised.[28]

It was measured that the absorbance of the model Tb_2(*m*-ODO2A-dimer)$^{2+}$ or Tb_2L^{2+} complex with DPA was 25 times greater than that without DPA at the same concentration. Additional quantum yield (QY) determinations of the model Tb_2L^{2+} complex without and with DPA showed that the QY values increased from 0.21% without DPA to 2.65% with DPA.[36,37] These data confirmed that the emission brightness (enhancement) ratio to be 25 x 12 = 300 for the Tb_2L complexes with and without DPA.[38] This 300 times signal enhancement allowed convenient luminescence imaging at the later bioimaging stage (*vide infra*).

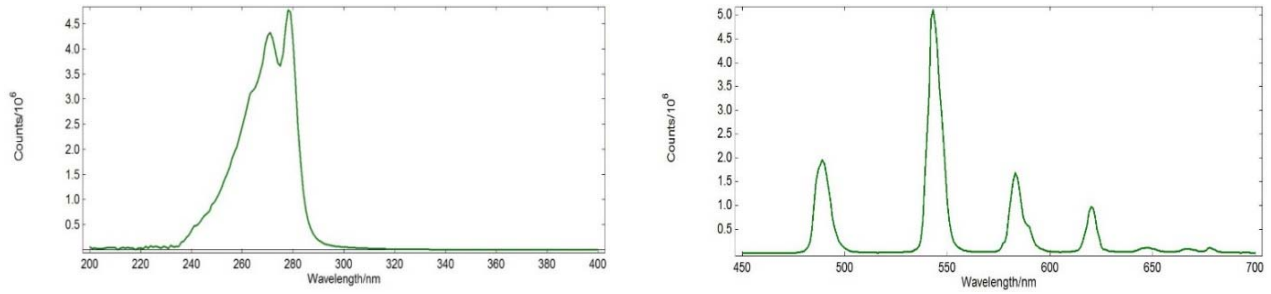

Figure 2. The excitation (λ_{em} = 544 nm, left) and emission (λ_{ex} = 278 nm, right) spectra of the complex 1, Tb_2(cRGDfK-ODO2A-dimer)$(DPA)_2$, 0.1 mM, pH 7.4, MOPS buffer.

Tb_2(*m*-ODO2A-dimer)$^{2+}$-DPA^{2-} binary complex binding studies.[30,39] Because of the limited amount of the Tb_2(cRGDfK-ODO2A-dimer)$^{2+}$ complex available, the analogous model complex Tb_2(*m*-ODO2A-dimer)$^{2+}$ or Tb_2L^{2+} (L = *m*-ODO2A-dimer) was used as a structural and bonding model for the DPA^{2-} ion binding studies. A luminescence titration of the Tb_2L^{2+} complex (λ_{ex} = 278 nm, λ_{em} = 544 nm) by the DPA^{2-} ion at pH 7.4 showed a saturation curve (Figure 3, left) with a break point at 2 equivalents of DPA added, indicating that the molecular formula of the adduct was $Tb_2L(DPA)_2^{2-}$. This is consistent with that each ODO2A macrocycle in the ditopic ligand occupied 6 coordination sites of the 9-coordinated Tb^{III} ion, leaving 3 meridional coordination sites for the tridentate DPA^{2-} ion to bind.[28,30] Taking the data between 1 and 3 equivalents of DPA added and fitting them to a two-site saturation ligand binding model gave two identical log K binding constants of 5.38, i.e. $K = 1/K_{d1} = 1/K_{d2}$ (R^2=0.996; Equation 1, where B_{max1} and B_{max2} are the maximum specific bindings to the two sites in the same units as Y, K_{d1} and K_{d2} are the equilibrium DPA dissociation constants). This binding constant value was about 0.38 log K unit lower than that of the more precise value determined by a more rigorous method (*vide infra*).

$$Y = B_{max1}*[DPA]/(K_{d1}+[DPA]) + B_{max2}*[DPA]/(K_{d2}+[DPA]) \quad (1)$$

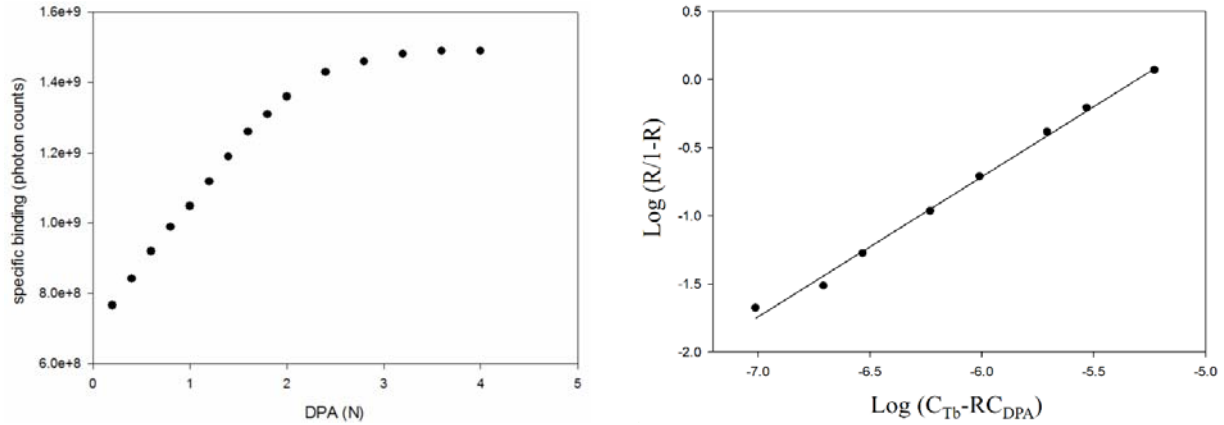

Figure 3. Left: Luminescence titration curve of 5 μM Tb_2(*m*-ODO2A-dimer)$^{2+}$ by DPA^{2-} ion (N = equivalent) at pH 7.4 (MOPS buffer, 25℃). Right: Plot of log(C_{Tb} – RC_{DPA}) *vs*. log (R/(1 – R)) for the

binary Tb_2(m-ODO2A-dimer)(DPA) complex, according to equation 3. [DPA^{2-}] = 100 nM, [Tb_2L^{2+}] = 50 – 5000 nM, pH 7.4 (MOPS/sodium acetate buffer), 25℃. λ_{ex} = 278 nm and λ_{em} = 544 nm were applied for the determination of Tb_2L(DPA) emission intensity.

A more rigorous method similar to that used by Jones and Vullev was employed to determine the first DPA^{2-} ion binding affinity with the Tb_2L^{2+} complex at pH 7.4, 25℃ (Equation 2, where L is the *m*-ODO2A-dimer ligand).[39] The binding affinity of the binary complex (K_1) was obtained using the linear relationship in Equation 3:[30]

$$Tb_2L^{2+} + DPA^{2-} \Leftrightarrow Tb_2L(DPA)\ ; \quad K_1 = [Tb_2L(DPA)]_{eq}/([Tb_2L^{2+}]_{eq}[DPA]_{eq}) \qquad (2)$$

$$\log(R/(1\text{-}R)) = \log(C_{Tb} - RC_{DPA}) + \log K_1\ ; \quad R = [TbDPA]_{eq}/([TbDPA]_{eq} + [DPA]_{eq}) \qquad (3)$$

where C_{Tb} is the total concentration of the Tb_2L^{2+} complex and R is the normalized integrated emission intensity. Thus, a linear plot of $\log(C_{Tb} - RC_{DPA})$ *vs*. log (R/(1 – R)) gave the respective slope and intercept values of 1.03±0.03 and log K_1 = 5.76±0.19 (R^2=0.995) for the binary Tb_2L(DPA) complex (Figure 3, right). To verify the method, a log K_1= 7.41±0.18 for the $Tb(DPA)^+$ complex was also determined by us using the same procedure which was in good agreement with the formation constant obtained by Jones and Vullev at a similar pH. The binding constant for the binary Tb_2L(DPA) complex was 1.65 log K units lower than that of the $Tb(DPA)^+$ complex which was probably due to some steric hindrance of the Tb^{III} binding sites in the macrocyclic ditopic complex. Interestingly, the fitting of the titration data of 100 nM DPA^{2-} ion by the Tb_2L^{2+} complex at pH 7.4 (MOPS buffer, 25℃) to a one-site saturation ligand binding model gave a log K_1 value of 5.60±0.42, which was only 0.16 log K unit lower than that obtained by the linear plot according to equation 3 (Figure S2, supporting information).

Note that in the previous study, the structural analogous heterodinuclear TbEu(*m*-ODO2A-dimer) or TbEuL complex was predicted to be in the "open-form" conformation in the pH range 6.7–10.6 assuming that the fluorescence energy transfer (FRET) between the Tb^{III} ion and the Eu^{III} ion could be characterized by the dipole-dipole mechanism.[21] Because the number of inner-sphere coordinated water molecules (q) of the Tb_2(cRGDfK-ODO2A-dimer) was determined to be 1.6~2.0, it was possible that both Tb_2L and the Tb_2(cRGDfK-ODO2A-dimer) complexes were in the "closed-form" conformation at pH 7.4. However, after the binding of the first DPA^{2-} ion to the Tb_2L^{2+} complex, the resulting Tb_2L(DPA) complex was most likely in the "open-form" conformation, making the second DPA^{2-} ion binding site similar to the first one. Thus, the second stepwise binding constant (log K_2) for the DPA^{2-} ion to result in the tertiary complex $Tb_2L(DPA)_2^{2-}$ was likely to be similar to or slightly but not much lower than 5.76. Assuming that the binary and tertiary DPA^{2-} binding constants of complex I were similar to those of the $Tb_2L(DPA)_2^{2-}$ complex, their binding

strength should be high enough to allow most of the DPA^{2-} ions remained coordinated at the sub-micromolar and higher concentrations of complex I for biological studies (*vide infra*, Figure 5).

$\alpha_v\beta_3$ integrin binding studies. To test whether the cRGDfK moiety in the dinuclear Tb^{III} complex was able to selectively bind $\alpha_v\beta_3$ integrin, receptor binding studies were carried out and compared with those of c(RGDfK)-FITC (a positive control) and Gly-ODO2A-dimer (a negative control). It was found that in the absence of added DPA molecules, the low intensity emission spectra of the Tb_2(cRGDfK-ODO2A-dimer)$^{2+}$ and the Tb_2(Gly-ODO2A-dimer)$^{2+}$ were not very much different from noise (Figure S3, supporting information). However, in the presence of added DPA^{2-} ions, the spectral peak intensities of the complex I (Figure 4, left, cyan) were distinctly greater than those of the Tb_2(Gly-ODO2A-dimer)$(DPA)_2^{2-}$ complex (Figure 4, left, brown).

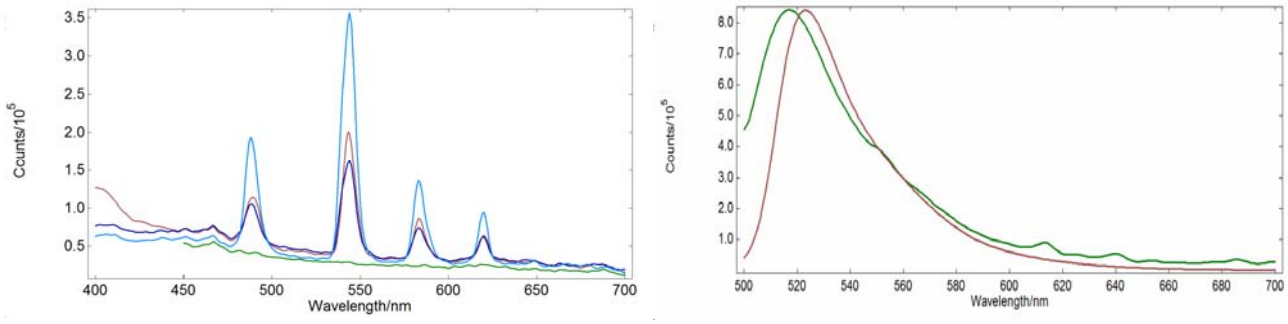

Figure 4. Left: Emission spectra of $\alpha_v\beta_3$ integrin binding with various reagents at 0.1 mM, λ_{ex} = 278 nm, pH 7.4, D-PBS buffer. Green: blank (D-PBS buffer only); cyan: complex I; brown: Tb_2(Gly-ODO2A-dimer)$(DPA)_2$; blue: complex I with 20 fold cRGDfK. Right: Emission spectra of c(RGDfK)-FITC (green) and FITC (brown), λ_{ex} = 492 nm, 0.1 mM.

The luminescence signals for the Tb_2(Gly-ODO2A-dimer)$(DPA)_2^{2-}$ complex were probably due to its non-specific binding with $\alpha_v\beta_3$ integrin and/or BSA in the blocking buffer solution. If 20 fold of cRGDfK was added to compete against the complex I for binding with $\alpha_v\beta_3$ integrin, the emission peak intensities were notably decreased to lower than but close to those of the Tb_2(Gly-ODO2A-dimer)$(DPA)_2^{2-}$ complex (Figure 4, left, blue). This confirmed the specific binding of complex I to $\alpha_v\beta_3$ integrin, and that there was also non-specific binding of complex I with $\alpha_v\beta_3$ integrin which was likely lower than or close to that of the Tb_2(Gly-ODO2A-dimer)$(DPA)_2^{2-}$ complex. It was difficult to distinguish if the non-specific binding for the Tb_2(Gly-ODO2A-dimer)$(DPA)_2^{2-}$ complex was due to its binding with the $\alpha_v\beta_3$ integrin and/or BSA in the blocking buffer solution, nor which part of the Tb_2(Gly-ODO2A-dimer)$(DPA)_2^{2-}$ complex, i.e. the Gly-part or the Tb_2(ODO2A-dimer)$(DPA)_2$-part, was involved. However, given the larger size of the Tb_2(ODO2A-dimer)$(DPA)_2$-part and the non-specific binding results observed above for the complex I, it was possible that the Tb_2(ODO2A-dimer)$(DPA)_2$-part of the complex was most likely involved in the non-specific binding. This non-specific binding was likely the reason for the large error bars observed from biological binding

studies at higher concentrations (*vide infra*, Figure 5). Figure 4 (right) showed that the cRGDfK-FITC as the $\alpha_v\beta_3$ integrin positive binding control exhibited a characteristic emission band at 517 nm which was similar to that of the FITC without cRGDfK. Note that the 517 nm emission band of cRGDfK-FITC was with a similar intensity as compared with that of the complex I at 544 nm, i.e. $3.2x10^5$ vs. $3.5x10^5$ photon counts.

Tumor cell binding studies. The human glioblastoma U87MG cells were used as the $\alpha_v\beta_3$ integrin-containing cells for the selective receptor binding and competition experiments.[40] The bound Tb_2(cRGDfK-ODO2A-dimer)$(DPA)_2^{2-}$ complex ions were determined using a previously constructed calibration curve (dynamic range 0.01-12.0 μM, r^2=0.9994; Figure S4, supporting information). The binding curve was shown in Figure 5 (left). A K_d value 19±10 μM was obtained. Comparing with those of cRGDfK-DOTA and cRGDfK-IRDye800 on either cell-based or protein-based $\alpha_v\beta_3$ integrin binding using NIR or fluorescence polarization competition assays,[19] our K_d value was one or two orders of magnitudes greater which might be due to different assay techniques employed and/or the steric hindrance imposed on the resulting complex I bioconjugate with a short spacer, similar to that reported for the structural analogous FITC-RGD_2 without galactose or polyethylene glycol (PEG) spacer.[20] Another possible reason for the low binding affinity of complex I with cell surfaces might be due to its hydrophilic nature which probably bound less strongly than the more lipophilic IRDye800 dye molecule, particularly at higher concentrations.

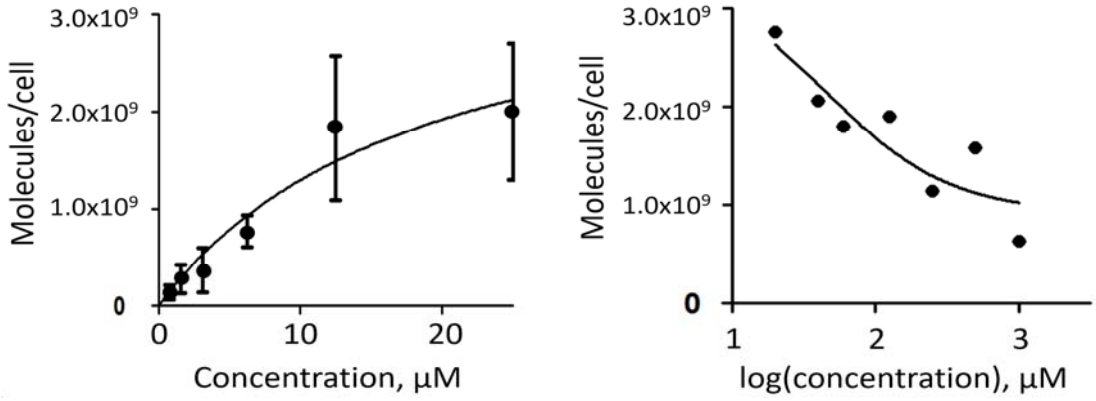

Figure 5. Left: binding curve of various added amounts of complex I (x-axis) towards U87MG cells. Right: competition of various added amounts of cRGDfK (x-axis) against 10 μM complex I toward U87MG cell binding.

In the cell competition binding experiments, various amounts of cRGDfK were added to compete against 10 μM complex I for binding with U87MG cells. Figure 5 (right) showed that the numbers of bound complex I molecules were decreased as the competing cRGDfK concentrations were increased. A value of IC_{50} 45 μM was obtained which was 4.5 times of the complex I concentration used, this ratio was comparable to that found for the cRGDfK-IRDye800.[19] Thus, the

specific binding of complex I toward U87MG cells *via* binding to $\alpha_v\beta_3$ integrin was reasonably confirmed.

Tumor cell imaging studies. The results of the confocal targeting U87MG cell imaging studies were shown in Figure 6.

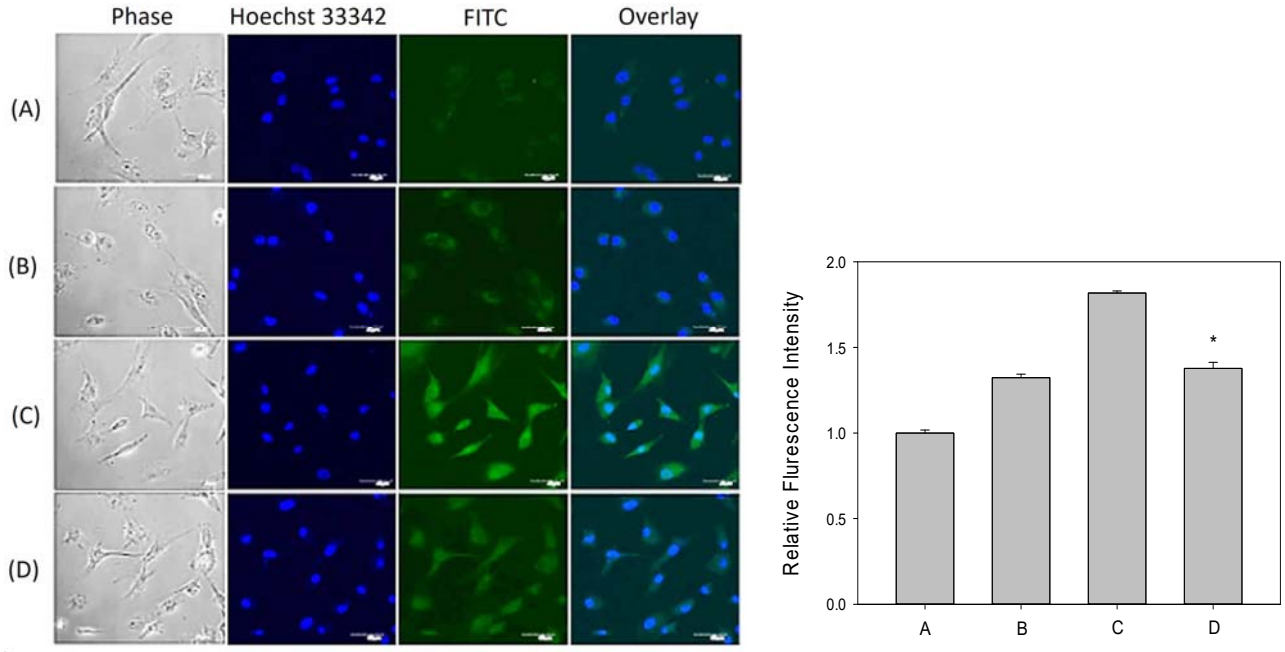

Figure 6. Left: 60X U87MG confocal cell imaging results: (A) Control (D-PBS and U87MG cells only), (B) complex I (25 μM), (C) cRGDfK-FITC (5 μM), (D) cRGDfK-FITC (5 μM) + complex I (25 μM). Right: relative fluorescence intensities. *The statistical P values were all smaller than 0.05 or even lower between any pair of intensity values in A-D.

In the absence of a suitable excitation laser source at 278 nm for the complex I molecule, we designed a competition protocol using cRGDfK-FITC (λ_{ex} = 492 nm) to demonstrate the specific binding of complex I toward U87MG cells (Figure 6, left). Figure 6A showed the images of the control (D-PBS and U87MG cells only) with the background fluorescence. Figure 6B showed the images of the complex I with U87MG cells which showed some residual green fluorescence. Figure 6C showed that after cRGDfK-FITC binding with U87MG cells, clear green FITC fluorescence was observed. Figure 6D was the result of 25 μM of complex I in competition against 5 μM of cRGDfK-FITC for U87MG cell binding, and it was seen that the fluorescence intensity was reduced. Quantitative treatment using the control data as background, the relative fluorescence intensities of the other three studies were all found to be greater than the background (Figure 6, right). The competition intensity (Figure 6D) was slightly greater than that of complex I with U87MG cells without competition (Figure 6B) indicating that there was still residual amount of cRGDfK-FITC left without being competed away. Thus, the specific binding between complex I with U87MG cells were

further demonstrated.

It is worthwhile to note that most luminescence cell binding and imaging experiments were performed at a complex I concentration range from sub-micromolar to 0.1 mM, and most of the DPA ligand likely remained coordinated to the Tb^{III} ion in the complex I as evidenced by the high luminescence signals and the linear calibration curve responses in the 0.01-12.0 μM concentration range. Because the excitation at 278 nm is far shorter than the biological window, complex I at present could most probably be used for preclinical *in vitro* bioimaging studies, perhaps in conjunction with Auger electron emitting Ln^{III} or In^{III} nuclides for theranostic investigations.[22] For future studies, in addition to reducing the non-specific binding, It would be helpful to design Ln^{III} chelates or other substances such as nanocomposites with longer wavelength excitation (e.g. λ_{ex} > 380 nm or preferably in the near infrared region) [41-43] or X-ray[44] excitation for more convenient, deep-penetrating *in vivo* bioimaging applications.

Conclusion

In conclusion, we have successfully prepared the dinuclear macrocyclic complex Tb_2(cRGDfK-ODO2A-dimer)$(DPA)_2^{2-}$ or complex I, *in situ*. At pH 7.4, complex I showed 300 times luminescence enhancement at 544 nm as compared to that without adding DPA (λ_{ex} = 278 nm). Complex I was found to bind to $\alpha_v\beta_3$ integrin and human glioblastoma U87MG tumor cells in both specific and non-specific modes, *via* fluorescence spectroscopic and confocal cell imaging competition studies. This makes complex I and its future optimized derivatives potentially feasible for preclinical *in vitro* and *in vivo* bioimaging applications, particularly in the time-resolved mode.

Experimental Section

Materials and Standard Solutions. Analytical reagent-grade chemicals and buffers, unless otherwise stated, were purchased from Sigma (St. Louis, MO, USA), Aldrich (Milwaukee, Wl, USA) or Merck (Darmstadt, Germany) and were used as received without further purification. Disodium ethylenediaminetetraacetic acid (Na_2H_2EDTA) was purchased from Fisher. The ligand *m*-ODO2A-dimer (1,3-bis[4,10-bis(carboxymethyl)-1,4,10-triaza-7-oxa-cyclododec-1-ylmethyl]benzene) was prepared and purified according to a published method.[21] The ligand cRGDfK-ODO2A-dimer was prepared and purified as described below. Carbonate-free deionized water (ddH_2O) was used for all solution preparations.

The concentrations of the *m*-ODO2A-dimer and cRGDfK-ODO2A-dimer stock solutions (ca. 0.01 M) was determined by pH titration using a standard tetramethylammonium hydroxide (TMAOH) solution (0. 1 M), with and without an excess of added Zn^{II} salt (i.e. $[Zn^{2+}] \geq 2.0[L]$). The concentration of the Tb^{III} nitrate stock solution was ca. 0.01 M and were standardized by EDTA titration using xylenol orange as indicator. The EDTA solution was standardized by titrating a

calcium carbonate primary standard solution (first dissolved in HCl solution) at pH 10 using calmagite as the indicator.

Solutions of Tb_2(*m*-ODO2A-dimer)$^{2+}$, Tb_2(cRGDfK-ODO2A-dimer)$^{2+}$, Tb_2(Gly-ODO2A-dimer)$(DPA)_2^{2-}$ and complex I were prepared by mixing two equivalents of Tb^{III} ions with one equivalent of the appropriate ligand with or without additional two equivalents of DPA and the final mixtures were slowly adjusted to pH 7.4 using the 3-(N-morpholino) propanesulfonic acid (MOPS) buffer solution (0.10 M). Mass spectrometry confirmed the presence of Tb_2(cRGDfK-ODO2A-dimer)$^{2+}$: $[M-H]^+$ calc. for $Tb_2C_{60}H_{88}N_{16}O_{10}S^+$, 1654.36, found 1654.70.

The 0.1 M $(CH_3)_4NOH$ solution was prepared by diluting a 25% $(CH_3)_4NOH$-aqueous solution obtained from Aldrich (carbonate-free) and was standardized by using reagent grade primary standard potassium hydrogen phthalate. A 0.1 M HCl solution was prepared by diluting a reagent grade HCl solution and standardized by using the standard $(CH_3)_4NOH$ solution. A 1.0 M stock solution of $(CH_3)_4NCl$ (Aldrich) was prepared and diluted to 0.1 M for each titration to maintain a constant ionic strength.

Mass Spectral Measurements. Mass spectrometric analyses were performed by the Center for Advanced Instrumentation and Department of Applied Chemistry at National Chiao Tung University, Hsinchu, Taiwan, R.O.C. Mass spectra of the Tb^{III}-cRGDfK-ODO2A-dimer complex solutions at pH 7.5 were acquired by direct infusion (2 μL). ESI(+)-MS experiments were carried out using an Impact HD Q-TOF mass spectrometer (Bruker, Germany) equipped with an electrospray ionization (ESI) source operating in positive ion mode. The parameters of ESI(+) included 4.5kV for ion spray voltage, 200°C for capillary temperature, and 6 L/min for sheath gas flow rate. The mass spectra were collected over the mass range of m/z 400 –3000 at a resolving power of 40000. The collected data were analyzed using Compass DataAnalysis 4.1 (Bruker, Germany).

Luminescence Measurements. Steady-state luminescence measurements were carried out on an Edinburgh Instruments FSP920 fluorescence system equipped with a 450W xenon arc lamp as the illumination source (λ_{ex} 278 nm, λ_{em} 544 nm). Emission light was collected into a TMS300 Czerny-Turner configuration double grating monochromator and detected by a Hamamatsu R928P photomultiplier tube in the visible wavelength range. Spectra were recorded by use of F900 Fluorescence spectrometer software. Luminescence decay curves were recorded by use of a μF920H flashlamp (Lamp Frequency: 100Hz) as the excitation source with the multiple-channel single photon counting mode (MCS). Data points from 0.1-0.2 half-life up to 4.5-5.5 half-lives were fitted by a nonlinear least-squares iterative technique (Marquardt-Levenberg algorithm) to obtain exponential decay half-life (τ) values. The average values of 2-3 measurements from different samples were reported.

For the Tb^{III}-*m*-ODO2A-dimer and Tb^{III}-cRGDfK-ODO2A-dimer solutions, all solutions were prepared from stock solutions of $Tb(NO_3)_3$ (~0.01M), *m*-ODO2A-dimer and cRGDfK-ODO2A-dimer (~0.01M). The molar ratio of the Tb^{3+} ion and the *m*-ODO2A-dimer or cRGDfK-ODO2A-dimer ligand was *ca*. 1.99:1.00 (2Tb-L) to make sure that the ligand was in slight excess. The pH of each solution was adjusted to desired value by adding 0.1 M $(CH_3)_4NOH$ solution and appropriate MOPS buffer solutions. All solutions were allowed to equilibrate overnight prior to luminescence measurements. The corresponding numbers of inner-sphere coordinated water molecules (q) were estimated using the lifetime data in H_2O and D_2O with established empirical equations.[28] The absorbance ratio and the quantum yields of the Tb_2(*m*-ODO2A-dimer) complexes without and with DPA were determined by using a published method and checked by the determination of that of Rhodamine B in H_2O to be 31% which was exactly the same as that reported.[36-38] All experiments were repeated and data checked at least twice carefully.

Additional luminescence titrations were performed by adding increasing small amounts (i.e. μL quantities) of standard dipicolinic acid (DPA, 1.0 mM) into a 2.0 mL, 5 μM Tb_2(cRGDfK-ODO2A-dimer) solution (pH 7.4, MOPS buffer) and the luminescence intensities were recorded after ~5 min equilibration time, and plotted against the added quantities of DPA. Sigma plot was used to analyze the titration data.

Synthesis of 3, 5-bis-hydroxymethylnitrobenzene and 3, 5-bis-bromomethylnitrobenzene. The two compounds were synthesized and characterized using the published procedures. The overall yield was ≥ 70%.[34]

Synthesis of 1-oxa-4,7,10-triazacyclododecane ($12N_3O$), and tricyclo[8,2,1,0]1-oxa-4,7,10-triazacyclotridecane ($12N_3O$-tricyclic). The two compounds were synthesized and characterized using the methods similar to the published procedures. The overall yield was ≥ 50%.[32,33]

Synthesis of 1,3-bis(1,4,10-triaza-7-oxacyclododec-1-ylmethyl)-5-nitro benzene (nitro-$12N_3O$-tricyclic-dimer).[34] In a rounded bottle flask containing 0.0073 mol $12N_3O$-tricyclic in 10 mL dry acetonitrile was added 0.90 g (0.0029 mol) 1,3-bis(bromomethyl)-5-nitrobenzene in 4 mL dry acetonitrile dropwise under a N_2 gas atmosphere with stirring. The mixture was heated at 50℃ for 6 h and cooled to room temperature. The white solid product was washed 3 times with dry acetonitrile. Yield 75.8%. NMR (D_2O, 400 MHz): ^1H: δ2.91, δ3.21, δ3.36, δ3.45, δ3.66, δ3.96, δ5.03, δ5.72, δ8.40, δ8.80; ^{13}C: δ50.12, δ50.73, δ58.13, δ63.41, δ69.01, δ106.11, δ129.83, δ131.07, δ142.29, δ149.03.

Synthesis of 1,3-bis(1,4,10-triaza-7-oxacyclododec-1-ylmethyl)-5-nitro benzene (nitro-$12N_3O$-dimer).[33] In a rounded bottle flask containing 0.25 g (0.00048 mol) $12N_3O$ tricyclic-dimer in 7 ml 2N NaOH was added 10 mL ethanol and the mixture was refluxed at 80℃ for 16 h and cooled

to room temperature. The mixture was extracted with chloroform and the chloroform extract was dehydrated with $MgSO_4$, filtered, and the yellow powder product was obtained by evaporation of the solvent. Yield 83.3%. NMR ($CDCl_3$, 400 MHz): 1H: δ2.56, δ2.62, δ2.72, δ3.57, δ3.63, δ7.50, δ7.97; 13C: δ44.49, δ46.57, δ51.87, δ58.82, δ66.47, δ122.90, δ135.82, δ141.14, δ148.38.

Synthesis of 1,3-bis[4,10-bis(carboxymethyl)-1,4,10-triaza-7-oxacyclododec-1-ylmethyl]-5-nitrobenzene hydrochloride salt (nitro-ODO2A-dimer, HCl salt).[32,33] In a rounded bottle flask containing 0.50 g (0.001 mol) nitro-12N_3O-dimer in 10 mL ddH_2O was added 5 equivalents bromoacetic acid and 6N NaOH to adjust and maintain the solution pH ~ 11 at 65℃ for 5 h. After the reaction, the solution was cooled to room temperature and was added 6N HCl to adjust pH to ~3. The solution was evaporated to almost dryness and the white NaCl solid was filtered and washed with 30 mL methanol. The filtrate was evaporated to dryness and re-dissolved in 3 mL ddH_2O and the pH was adjusted to 1 by adding 6N HCl. The white product was purified by passing through a cation exchange column in the H^+ form and evaporated to dryness. Yield 67.5%. NMR (D_2O, 400 MHz): ^{1}H: δ2.99, δ3.59, δ3.85, δ3.89, δ3.94, δ7.74, δ8.16; ^{13}C: δ46.8, δ51.9, δ55.1, δ55.3, δ55.8, δ64.0, δ125.1, δ137.8, δ138.7, δ148.2, δ168.1. $[M+H]^+$ calc. for $C_{32}H_{51}N_7O_{12}^+$, 725.79, found 726.3. (Supporting Information)**.**

Synthesis of 1,3-bis[4,10-bis(carboxymethyl)-1,4,10-triaza-7-oxacyclododec-1-ylmethyl]-5-aniline hydrochloride salt (amine-ODO2A-dimer, HCl salt). In a rounded bottle flask containing 0.10 g (0.102 mmol) nitro-ODO2A-dimer in 18 ml ddH_2O was added 22 mg Pd/C and stirred for 2 h under a H_2 atmosphere. The solution was filtered with celite and washed several times with ddH_2O. The filtrate was evaporated to dryness, dissolved in small amount of ddH_2O and purified by passing through a cation exchange column in the H^+ form. The light yellow product was obtained by evaporation the eluate to dryness. Yield 78.9%. NMR (D_2O, 400 MHz): ^{1}H: δ2.98, δ3.59, δ3.81, δ3.91, δ3.93, δ7.39, δ7.49; ^{13}C: δ47.1, δ51.8, δ55.0, δ55.8, δ56.0, δ64.0, δ124.9, δ130.6, δ132.8, δ138.2, δ168.5. ESI-MS, $[M+H]^+$ calc. for $C_{32}H_{33}N_7O_{10}^+$, 696.4, found 696.3. (Supporting Information).

Synthesis of 1,3-bis[4, 10-bis(carboxymethyl)-1,4,10-triaza-7-oxacyclododec-1-ylmethyl]-5-isothiocyanatobenzene, hydrochloride salt (SCN-Bn-ODO2A-dimer, HCl salt).[35] In a rounded bottle flask containing 0.13 g (0.158 mmol) amine-ODO2A-dimer in 5 mL ddH_2O was added 0.36 mL (0.47 mmol) thiophosgene ($CSCl_2$) in 5 mL $CHCl_3$ and stirred for 3 h at room temperature. After the reaction, the aqueous layer was separated from the organic layer, and the organic layer was extracted with small amounts of ddH_2O three times and the combined aqueous layer was evaporated to dryness to obtain the yellow product. Yield 70%. NMR (D_2O, 400 MHz): ^{1}H: δ3.07, δ3.66, δ3.83, δ3.98, δ4.00, δ7.34, δ7.37; ^{13}C: δ47.1, δ52.0, δ55.1, δ55.6, δ56.1, δ64.3, δ127.5, δ131.2, δ 132.0, δ136.2, δ137.5, δ168.3. ESI-MS, $[M+H]^+$ calc. for $C_{33}H_{52}N_7O_{10}S^+$, 738.9, found 738.3.(Supporting Information).

Synthesis of cRGDfK-ODO2A-dimer.[35] The compounds SCN-Bn-ODO2A-dimer (1.1067 mg, 0.0015 mmol) and cRGDfK (i.e. cyclo[Arg-Gly-Asp-d-Phe-Lys], 1.812 mg, 0.003 mmol) were added into 1 mL 0.1 M sodium carbonate-bicarbonate buffer solution (pH 9.0) and the mixture was stirred for 1 day at room temperature. The reaction completion was checked by a HPLC procedure and the final cRGDfK-ODO2A-dimer product was purified by a similar FPLC method. Yield 84%. MALDI-TOF MS, $[M+H]^+$ calc. for $C_{60}H_{93}N_{16}O_{17}S^+$, 1342.562, found 1341.637. (Supporting Information).

Synthesis of Gly-ODO2A-dimer. The compounds SCN-Bn-ODO2A-dimer (3.69 mg, 0.005 mmol) and glycine (3.75mg, 0.05 mmol) were added into 1 mL 0.1 M sodium carbonate-bicarbonate buffer solution (pH 9.0) and the mixture was stirred for 1 day at room temperature. The reaction completion was checked by a HPLC procedure and the final product was purified by a similar FPLC method. (Supporting Information).

Synthesis of cRGDfK-FITC. The compounds cRGDfK (0.905 mg, 0.0015 mmol) and FITC (1.168mg, 0.003 mmol) were added into 1 mL 0.1 M sodium carbonate-bicarbonate buffer solution (pH 9.0) and the mixture was stirred for 1 day at room temperature. The reaction completion was checked by a HPLC procedure and the final product was purified by a similar FPLC method. ESI-MS, $[M+H]^+$ calc. for $C_{48}H_{53}N_{10}O_{12}S^+$, 994.07, found 993.5. (Supporting Information).

Tb^{3+}/Tb_2(m-ODO2A-dimer)$^{2+}$-DPA binary complex binding studies. Association constants for Tb^{3+} and Tb_2(m-ODO2A-dimer)$^{2+}$ to DPA^{2-} ion were determined *via* titration of Tb^{3+} and Tb_2(m-ODO2A-dimer)$^{2+}$ from 50 nM up to 5 μM against 100 nM DPA in 0.2 M sodium acetate (pH 7.4, MOPS buffer, 25°C). A linear fit similar to that of the one-step equilibrium model of Jones and Vullev[33] was applied as the concentrations of Tb^{3+} and Tb_2(m-ODO2A-dimer)$^{2+}$ were mostly greater than $[DPA^{2-}]$, and the binding affinity of the binary complex (K_1) was obtained using the following linear relationship[27]:

$$\log(R/(1-R)) = \log(C_{Tb} - RC_{DPA}) + \log K_1; \quad R = [TbDPA]_{eq}/([TbDPA]_{eq} + [DPA]_{eq}) \qquad (3)$$

where C_{Tb} is the total concentration of the Tb^{3+} ion or the Tb_2(*m*-ODO2A-dimer)$^{2+}$ complex and R is the normalized integrated emission intensity. Thus, a plot of $\log(C_{Tb} - RC_{DPA})$ *vs*. $\log(R/(1-R))$ will produce a linear fit with a slope of unity and a y-intercept equal to the logarithm of K_1.

Protein binding experiments. The $\alpha_v\beta_3$ integrin (500 ng/mL) was added into the plastic cuvets for 16 h at 4℃, followed by washing 3 times with Dulbecco's phosphate-buffered saline (D-PBS) buffer. To the cuvets was then added 3% bovine serum albumin (BSA) blocking buffer and allowed to stand for 1 h. After washing, to each cuvet was separately added 2.5 mL 100 μM of Tb_2(cRGDfK-ODO2A-dimer)$^{2+}$, Tb_2(Gly-ODO2A-dimer)$^{2+}$ and Tb_2(cRGDfK-ODO2A-dimer)$(DPA)_2^{2-}$ (without and with 2 mM c(RGDfK)), Tb_2(Gly-ODO2A-dimer)$(DPA)_2^{2-}$ and c(RGDfK)-FITC, and each cuvet

solution was allowed to equilibrate for 2 h. Each curvet was then washed 3 times with D-PBS and the fluorescence emission spectrum was measured. All tests were repeated at least 3 times.

Cell binding experiments. The cells were cultivated in Minimum Essential Medium alpha (MEM-α) with 10% fetal bovine serum (FBS), 1% penicillin streptomycin (PS) at 5% carbon dioxide/air, 37°C. For the U87MG cell binding experiments, 1×10^6 U87MG cells were suspended in the centrifuge tubes and fixed with 4% paraformaldehyde for 10 min at 25℃. The tube solutions were washed with D-PBS and then added protein-free blocking reagent for 1 h, and washed again with D-PBS. Various amounts of Tb_2(cRGDfK-ODO2A-dimer)$(DPA)_2^{2-}$ complex were added and the tube solutions were allowed to equilibrate for 2 h at 25℃, and then washed with D-PBS to remove the unbound Tb_2(cRGDfK-ODO2A-dimer)$(DPA)_2^{2-}$ complex. After counting the number of cells in each tube,[34] the cell solutions were transferred into a quartz cell for luminescence spectral measurements to determine the bound Tb_2(cRGDfK-ODO2A-dimer)$(DPA)_2^{2-}$ molecules, using a previously constructed calibration curve (dynamic range 0.01-12.0 μM, r^2=0.9994; Figure S3, supporting information). In the cell competition binding experiments, various amounts of cRGDfK were added to compete against 10 μM complex I for binding with U87MG cells. The bound Tb_2(cRGDfK-ODO2A-dimer)$(DPA)_2^{2-}$ molecules were determined in the similar ways as that of the normal cell binding studies. The binding curves and K_d and IC_{50} values were obtained using the GraphPad Prism 5.0 software.

Confocal targeting U87MG cell imaging studies. Cover glass plates were treated with poly-D-lysine and washed with PBS buffer before adding 3×10^5 U87MG cells for 1 day with the cultivation medium. The plates were then washed with PBS buffer and the cells were fixed by adding 4% paraformaldehyde solution (pH 7.4) for 10 min and washed with PBS buffer again. After the addition of protein-free blocking reagent for another 1 h and washing with D-PBS buffer, the plates were added four different test reagent solutions to react for 1 h. With D-PBS buffer washing and Hoechst 33342 (1:1000) cell nuclei dyeing for 10 min and D-PBS buffer washing, the plates were examined by the Olmpus FV10i microscope after mounting medium treatment.

Acknowledgements. Financial supports from the Ministry of Science and Technology of Taiwan, ROC (grant no. NSC-100-2811-M-010-003, NSC102-2627-M-010-001, and MOST103–2627-M-010–001) are acknowledged. Thanks are also due to Dr. J.-J. Li for helpful discussions. Mass spectrometric analyses were performed by the Center for Advanced Instrumentation and Department of Applied Chemistry at National Chiao Tung University, Hsinchu, Taiwan, R.O.C. We thank Dr. Sheng-Cih Huang and Ms. Yun-Ming Li (Mass Laboratory, National Chiao-Tung University, Hsinchu) for mass spectrometry analysis.

Funding Sources. Ministry of Science and Technology of Taiwan, ROC (grant no. NSC-100-2811-M-010-003, NSC102-2627-M-010-001, and MOST103–2627-M-010–001)

Supporting Information. Selected NMR spectra with peak assignments, HPLC chromatograms and mass spectra of various intermediates and SCN-Bn-ODO2A-dimer derivatives, luminescence decay curves of Tb_2(cRGDfK-ODO2A-dimer) without and with DPA and estimation of the number of coordinated water molecules (q), emission spectra of Tb_2(cRGDfK-ODO2A-dimer)$^{2+}$ and Tb_2(Gly-ODO2A-dimer)$^{2+}$, and calibration curve of Tb_2(cRGDfK-ODO2A-dimer)$(DPA)_2^{2-}$ are shown in the supporting information.

Abbreviations. DFT: density functional theory; DPA: dipicolinate ion; FITC: fluorescein isothiocyanate; FRET: fluorescence energy transfer; MOPS: 3-(N-morpholino) propanesulfonic acid; m-ODO2A-dimer: 1,3-bis[4,10-bis(carboxymethyl)-1,4,10-triaza-7-oxa-cyclododec-1-ylmethyl] benzene; SCN-Bn-ODO2A-dimer: 1,3-bis[4, 10-bis(carboxymethyl)-1,4,10-triaza-7-oxacyclododec-1-ylmethyl]-5-isothiocyanatobenzene.

References

1. E. Ruoslahti, M.D. Pierschbacher, *Science*, 1987, 238, 491-497.
2. J.S. Desgrosellier, D.A. Cheresh, *Nature Rev. Cancer*, 2010, 10, 9-22.
3. J. Folkman, *Nature Med.*, 1995, 1, 27-31.
4. D. Hanahan, J. Folkman, *Cell*, 1996, 86, 353-364.
5. G. Bergers, E. Laura, L.E. Benjamin, *Nature Rev. Cancer*, 2003, 3, 401-410.
6. N. Ferrara, R.S. Kerbel, *Nature*, 2005, 438, 967-974.
7. E. Pasquier, M. Kavallaris, N. André, *Nature Rev. Clin. Oncol.*, 2010, 7, 455-465.
8. P. Carmeliet, R.K. Jain, *Nature*, 2011, 473, 298-307.
9. H.M. Sheldrake, L.H. Patterson, *Curr. Cancer Drug Targets*, 2009, 9, 519-540.
10. S. Liu, *Mol. Pharmaceutics*, 2006, 3, 472-487.
11. F.K. Gaertner, H. Wester, M. Schwaiger, A. Beer, *Eur. J. Nucl. Med. Mol. Imaging*, 2012, 39, S126-S138.
12. P. Burke, S. DeNardo, L. Miers, K. Lamborn, S. Matzku, G. DeNardo, *Cancer Res.*, 2002, 62, 4263–4272.
13. R. Stupp, M.E. Hegi, T. Gorlia, et al. *Lancet Oncol.*, 2014, 15, 1100-1108.
14. S. Liu, *Bioconjugate Chem.*, 2015, 26, 1413–1438.
15. S. Liu. *Molecular Pharmaceutics*, 2006, 3, 472-487.
16. S. Liu. *Advanced Drug Delivery Reviews*, 2008, 60, 1347-1370.
17. S. Liu. *Bioconjugate Chemistry*, 2009, 20, 2199-2213.
18. T. Ito, M. Inoue, K. Akamatsu, E. Kusaka, K. Tanabe, S.-i. Nishimoto, *Bioorg. Med. Chem. Lett.*, 21, 3515-3518.
19. H.M. Shallal, S.R. Banerjee, A. Lisok, R.C. Mease, M.G. Pomper, *Bioconjugate Chem.*, 2014, 25, 393-405.

20. Y. Zheng, S. Ji, A. Czerwinski, F. Valenzuela, M. Pennington, S. Liu, *Bioconjugate Chem.*, 2014, 25, 1925-1941.
21. C.A. Chang, H.-Y. Lee, S.-L. Lin, C.-N. Meng, T.-T. Wu, *Chem. Eur. J.* 2018, 24, 6442-6457.
22. J.-J. Li; K.-L. Lan; S.-F. Chang, Y.-F. Chen, W.-C. Tsai, P.-H. Chiang, M.-H. Lin, W.B. Fischer, Y.-S. Shih, S.-H. Yen, R.-S. Liu, Y.-G. Tsay, H.-E. Wang, C.A. Chang, *Bioconjugate Chem.*, 2015, 26, 2481–2496.
23. J.-J. Li, S.-F. Chang, I.-I. Liau, P.-C. Chan, R.-S. Liu, H.-E. Wang, C.A. Chang, *J. Biomed. Sci.* 2016, 23, 15.
24. N. Gahlaut, L.M. Miller, *Cytometry A*, 2010, 77, 1113-1125.
25. J.-C.G. Bünzli, *Chem. Rev.* 2010, 110, 2729–2755.
26. N. Sabbatini, S. Perathoner, V. Balzani, B. Alpha, J.-M. Lehn, In *Supramolecular Chemistry*; V. Balzani, Ed.; D. Reidel Publishing Co.: Dordrecht, 1987.
27. C.A. Chang, in *Handbook on the Physics and Chemistry of Rare Earths*, Vol. 51 (Eds.: J.-C. G. Bünzli, V. K. Pecharsky), Elsevier, 2017, Ch. 297, pp. 169-299.
28. C.A. Chang, I.-F. Wang, H.-Y. Lee, C.-N. Meng, K.-Y. Liu, Y.-F. Chen, T.-H. Yang, Y.-M. Wang, Y.-G. Tsay, *Dalton Trans.* 2012, 41, 14697-14706
29. M.L. Cable, J. P. Kirby, H.B. Gray, A. Ponce, *Acc. Chem. Res.*, 2013, 46, 2576-2584.
30. M.L. Cable, J.P. Kirby, D.J. Levine, M.J. Manary, H.B. Gray, A. Ponce, *J. Am. Chem. Soc.*, 2009, 131, 9562-9570.
31. K.P. Nandre, S.V. Bhosale, K.V.S.R. Krishna, A. Guptac, S.V. Bhosale, *Chem. Commun.*, 2013, 49, 5444-5446.
32. Dischino, E. Delaney, J. Emswiler, G. Gaughan, J. Prasad, S. Srivastava, M. Tweedle, *Inorg. Chem.* 1991, 30, 1265-1269.
33. C. Gløgård, R. Hovland, S.L. Fossheim, A.J. Aasen, J.J. Klaveness, *Chem. Soc., Perkin Trans. 2*, 2000, 1047–1052.
34. M. Le Baccon, F. Chuburu, L. Toupet, H. Handel, M. Soibinet, I. Déchamps-Olivier, J.-P. Barbier, M. Aplincourt, *New J. Chem.* 2001, 25, 1168-1174.
35. D.N. Pandya, N. Bhatt, A.V. Dale, J.Y.; Kim, H. Lee, Y.S. Ha, J.-E. Lee, G.I. An, J. Yoo, *Bioconjugate Chem.*, 2013, 24, 1356-1366.
36. J. C. Boyer, F. C. Van Veggel, *Nanoscale*, 2010, 2, 1417-1419.
37. D. Magde, G.E. Rojas, and P. Seybold, *Photochem. Photobiol*, 1999, 70, 737-744.
38. N. C. Shaner, P. A. Steinbach, R. Y. Tsien, *Nat. Methods*, 2005, 2, 905909.
39. G. Jones, V.I. Vullev, *J. Phys. Chem. A* 2002, 106, 8213–8222.
40. S.A. Altman, L. Randers, G. Rao, *Biotechnol. Prog.*, 1993, 9, 671–674.
41. Y.O. Fung, W. Wu, C.-T. Yeung, H-K. Kong, K.K.-C. Wong, W.-S. Lo, G.-L. Law, K.-L. Wong, C.-K. Lau, C.-S. Lee, W.-T. Wong, *Inorg. Chem.*, 2011, 50, 5517-5525.
42. D. Arosio, L. Manzoni, E. M. V. Araldi, C. Scolastico, *Bioconjugate Chem.*, 2011, 22, 664–672.
43. S. Cui, D. Yin, Y. Chen, Y. Di, H. Chen, Y. Ma, S. Achilefu, Y. Gu, *ACS Nano*, 2013, 7, 676-

688.
44. C.-C. Hsu, S.-L. Lin, and C.A. Chang, *ACS Appl. Mater. Interfaces*, 2018, 10, 7859-7870.

Table of Contents Graphic

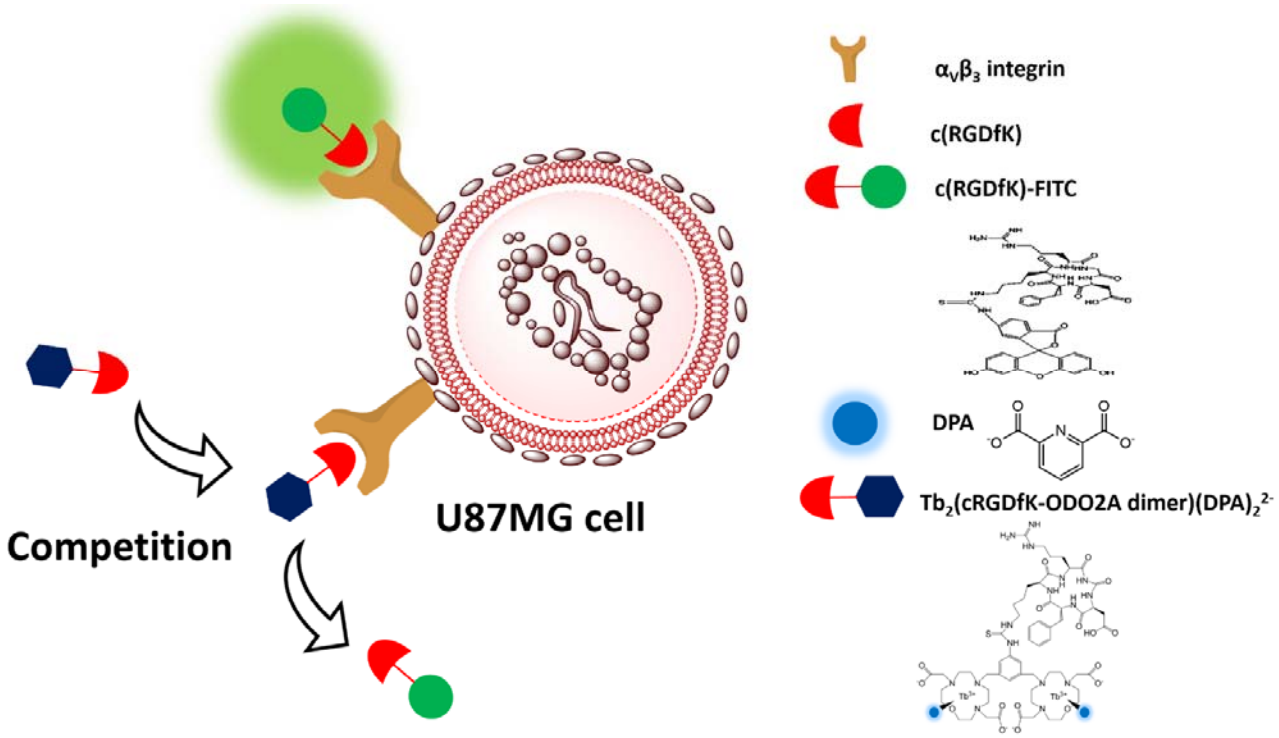

The cyclic-RGD dinuclear Tb^{III} macrocyclic complex Tb_2(cRGDfK-ODO2A-dimer)$(DPA)_2^{2-}$ at pH 7.4 showed 300 times luminescence (λ_{ex} = 278 nm) enhancement at 544 nm as compared to that without adding DPA and was found to selectively bind to $\alpha_v\beta_3$ integrin and human glioblastoma U87MG tumor cells *via* fluorescence spectroscopic and confocal cell imaging competition studies, making it potentially feasible for practical bioimaging applications, particularly in the time-resolved mode.

Keywords: Cyclic RGD; Dinuclear Tb^{III} macrocyclic complex; Luminescence probe; Integrin-selective binding; Intensity enhancement